Chapter 10
Topologically Complex Morphologies in Block Copolymer Melts

J. J. K. Kirkensgaard

Abstract Polymers are macromolecules built from chains of subunits. Most synthetic polymers are built from a single subunit, the monomer, and are termed homopolymers. The connection of two or more homopolymer chains into a larger macromolecule is termed a *block copolymer* and these can be made with multiple components connected into both linear or branched molecular architectures. Block copolymers remain a subject of significant research interest owing to the control and reproducibility of physical properties and the many fascinating nanoscale structures which can be obtained *via* self-assembly. The self-assembly behaviour of block copolymers originate from the tendency of the various polymer chains to undergo phase separation which is inherently constrained due to the molecular connectivity. This leads to the formation of ordered mesostructures with characteristic length scales on the order of the chain sizes, typically tens of nanometers. Here the focus is on the molecular architecture as a topological variable and how it influences the morphologies one finds in self-assembled block copolymer systems. We present a range of examples of morphologies with different and sometimes very complex mesoscale topology, i.e. patterns which emerges from the tendency of these molecules to undergo spatial phase separation.

10.1 Introduction

Polymers are macromolecules built from chains of subunits. Naturally occurring examples of polymers include DNA and proteins built from chains of nucleic and amino acids respectively or cellulose built from chains of connected glucose units. Most synthetic polymers are built from a single subunit, the monomer, and are termed

J. J. K. Kirkensgaard (✉)
Niels Bohr Institute, University of Copenhagen, Copenhagen, Denmark
e-mail: jjkk@nbi.dk

S. Gupta and A. Saxena (eds.), *The Role of Topology in Materials*,
Springer Series in Solid-State Sciences 189,
https://doi.org/10.1007/978-3-319-76596-9_10

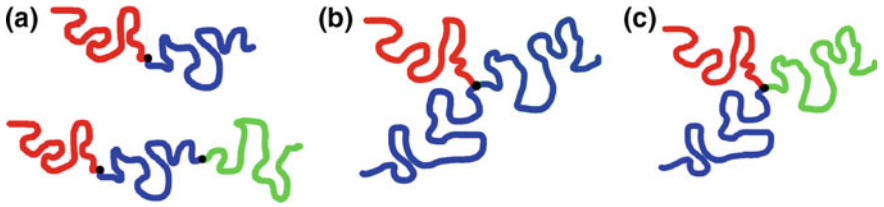

Fig. 10.1 Block copolymers. Covalent bonding of different polymer chains A, B, C, …results in block copolymers of varying molecular architecture, here **a** linear AB diblock copolymers and ABC triblock terpolymers, **b** star-shaped AB_2 miktoarm copolymer and **c** ABC star miktoarm terpolymer

homopolymers. The connection of two or more homopolymer chains into a larger macromolecule is termed a *block copolymer* and these can be made with multiple components connected into both linear or branched molecular architectures as illustrated in Fig. 10.1. Block copolymers remain a subject of significant research interest owing to the control and reproducibility of physical properties and the many fascinating nanoscale structures which can be obtained [1]. The self-assembly behavior of block copolymers originate from the tendency of the various polymer chains to undergo phase separation which is however inherently constrained due to the molecular connectivity. This leads to the formation of ordered mesostructures with characteristic length scales on the order of the chain sizes, typically tens of nanometers. The formation of ordered structures in block copolymer systems stems from a competition between two effects: the entropic penalty associated with chain stretching and compression causing a preference for domains with constant thickness, and an enthalpic penalty associated with interfacial energy causing a preference for domain shapes which minimise surface area. In equilibrium a compromise between these factors is achieved by forming interfacial surfaces which tend to have approximately constant mean curvature. The nanostructures described below represent a tremendous potential for future technological applications because they provide a bottom-up route to materials with tailored optical, mechanical, electrical and photovoltaic properties (and combinations thereof), for example through phase selective chemistries or selective sequential removal of the blocks.

In this chapter two notions of topology will be relevant: First we will talk about the topology of the macromolecules, i.e. the arrangement of chains in the individual copolymers, but we will use the term ‘molecular architecture’ to describe this. We will focus in detail on the molecular architecture as a topological variable and how it influences the morphologies one finds in self-assembled block copolymer systems. Secondly, we present a range of examples of morphologies with different and sometimes very complex mesoscale topology, i.e. patterns which emerges from the tendency of these molecules to undergo spatial phase separation under the constraint of the molecular connectivity and which show periodicities on the length scale of the chain sizes as described above. We will restrict ourselves to looking at polymer

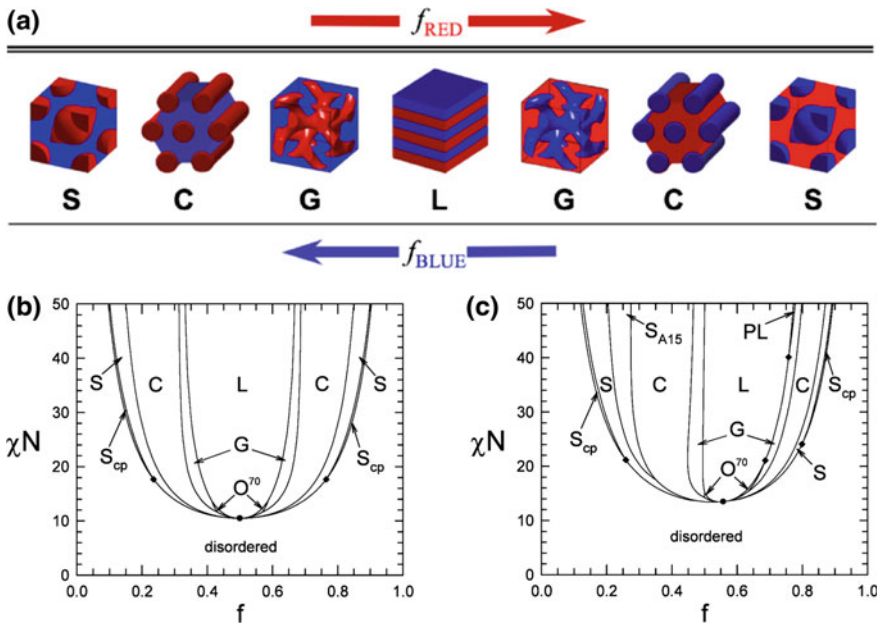

Fig. 10.2 Phase diagrams of AB-type block copolymers. **a** Morphologies found in AB diblock systems. S: cubic sphere packing, C: hexagonal cylinders, G: bicontinuous double gyroid, L: Lamellar. Figure from [2]. **b** Theoretical phase diagram for AB diblock copolymers. The O^{70} phase is an orthorhombic network phase described below. **c** Theoretical phase diagram for branched AB_2 miktoarm star copolymer. Phase diagrams from [3]

melts, i.e. polymers in a liquid state above the glass transition temperature without any added solvent.

10.2 AB Block Copolymers

The simplest block copolymers are AB diblocks where two polymer chains A and B are connected at a single junction point (see Fig. 10.1a). Diblock copolymers have been studied for decades and their self-assembly are generally well understood [3]. The structural phase behaviour of AB diblock copolymers is usually described as a function of two parameters: the composition, i.e. the relative volume fractions of the two components, and the degree of segregation described by the product χN where χ is the Flory-Huggins interaction parameter describing the chemical incompatibility between the different chains and N is the degree of polymerisation (the length of the polymer) [4, 5]. A characteristic feature of diblock copolymer self-assembly is that for increasing segregation, the phase behaviour becomes dominated by the com-

position. As a function of the composition described by the A component volume fraction $f = f_A$ ($f_B = 1 - f_A$) the universal phase diagram in the strong segregation limit consists of four ordered morphologies namely lamellar, bicontinuous double gyroid, hexagonally arranged cylinders and a cubic bcc sphere packing, all in principle appearing symmetrically around a 50/50 composition ($f = 0.5$). These phases are illustrated in Fig. 10.2a and a complete phase diagram based on a self-consistent field theory prediction is shown in Fig. 10.2b. The χ parameter for a given polymer pair is usually temperature dependent so that one can decrease the segregation by raising the temperature (and vice versa). This means that at $f = 0.4$ for example one should in principle be able to find phase transitions from L $\rightarrow$ G $\rightarrow$ C $\rightarrow$ disorder by increasing temperature (thus moving vertically in the phase diagram).[1] The latter is termed the order-disorder transition and the others order-order transitions. Inspection of the morphologies in Fig. 10.2a reveal that these phases are either based on simple topologies like planes, cylinders, spheres or in the case of the double gyroid, the more complex topology of networks whose midsurface is describable as a minimal surface [6]. Whichever it is, an order-order transition often necessitates a change of topology. Here we will not discuss such phase transitions in detail, but will rather focus on the effect of changing the molecular architecture and composition.

In Fig. 10.2c a phase diagram of two-component AB_2 miktoarm stars are shown. For a given composition quantified by f, the change in molecular architecture induces increased interfacial curvature leading to shifts in the phase diagram, increasing for example the regions of spherical packings by introducing the A15 phase (see Fig. 10.3) and also stabilising another new morphology, the perforated lamellae (PL) where lamellar sheets of the B-component is protruded by hexagonally arranged pillars of the majority matrix component A. Also, the O^{70} network phase exhibits a larger region on the $f > 0.5$ side of the diagram with the B-component forming the network and the A-component the matrix [3]. As we shall see below, changing the molecular architecture allows the formation of spectacular structures when increasing the number of components to more than two. The formation of low symmetry sphere packings is an ongoing topic in soft matter self-assembly [9] with a prominent example found in a block copolymer melt, namely the discovery of a large unit cell tetragonal structure known from metal alloys as the σ Frank–Kasper phase [8], see Fig. 10.3b, c. The low symmetry sphere packings like A15 and the σ phase are known as approximants to aperiodic quasicrystalline arrangements characterised by rotational symmetry, but not translational symmetry. The finding of the σ phase recently led to the discovery of a long-lived metastable dodecagonal quasicrystalline phase in a block copolymer system [10].

[1] There are a number of practical subtleties associated with this statement. First of all it requires that the molecular weight (or N) is not so large that the temperatures required to reach the transitions disintegrates the molecules, and second, the temperature range has to be above the glass transition temperature T_g which is a property of the specific chains. We will assume we are in a region of size and temperature where the notion of phase transitions makes sense. Note however that in structural studies of block copolymer morphologies one often utilises the glass transition of one or more of the chains to effectively 'freeze' a given structure by a rapid temperature quench.

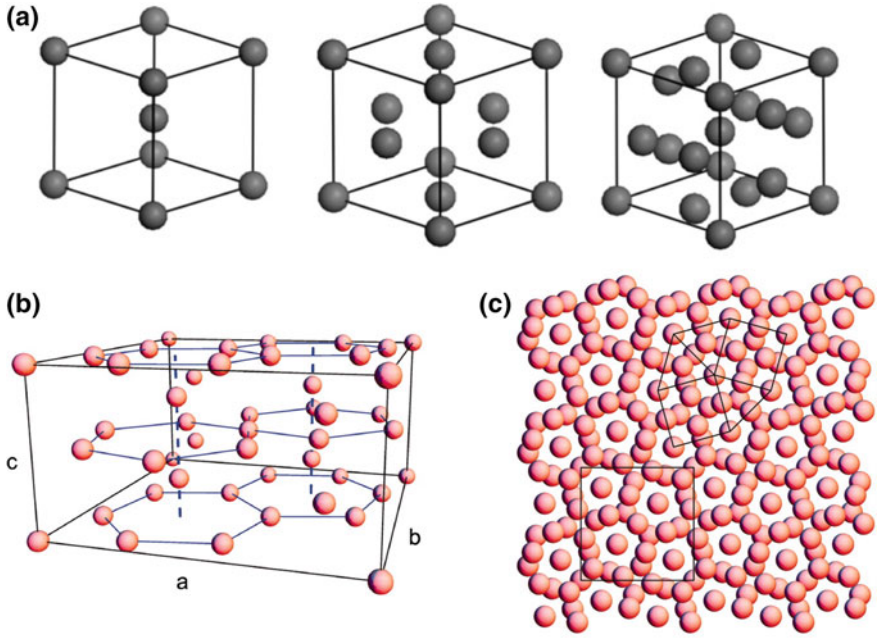

Fig. 10.3 Sphere packings found in block copolymer systems. **a** Cubic packings BCC, FCC and A15. Figure from [7]. **b, c** Frank–Kasper σ-phase. Figure from [8]

10.3 ABC Block Copolymers

The addition of a third component dramatically increases the morphological phase space as seen with linear ABC terpolymers where a large number of different structures have been found [1, 11]. A unifying feature between the structures formed in linear ABC systems and those found in simpler AB systems is that they are all characterised by the *interfaces* of each pair of polymer species. So speaking in terms of structural motifs, linear ABC block copolymers also explore variations of the surface topologies mentioned above: sphere, cylinder, plane, networks/minimal surface, but in multicolor versions, see Fig. 10.4 for a few examples. Nevertheless, the addition of a third component still allows more detailed control of the resulting morphologies and also opens up regions in the phase diagram of new and complex phases. An example is the poly(isoprene-b-styrene-b-ethylene oxide) linear triblock terpolymer system (ISO) studied experimentally and theoretically by Bates and colleagues [12] where several complex network phases are shown to form in the phase region between 2- and 3-colored lamellar structures, see Fig. 10.4b, c. The orthorhombic O^{70} phase is a single net structure while the Q^{230} and Q^{214} phases are both of the double gyroid type. The difference is the molecular packing: in the Q^{230} the nets are symmetric while in Q^{214} the two nets are built from different chemical species lowering the symmetry to the chiral subgroup since each of the double gyroid nets are chiral enantiomers (of

opposite handedness). The formation of network phases like the double gyroid is a well-known phenomena in soft matter self-assembly where it is found ubiquitously in for example lipid and surfactant systems forming lyotropic liquid crystals [6]. Here the 3-connected double gyroid appears as one of typically three phases formed, the others being the 4-connected double diamond phase and the 6-connected primitive phase - all of cubic symmetry. In pure AB and ABC linear block copolymer melts all network phases found is of the 3-connected kind which is ultimately a result of the configurational entropy loss associated with chain stretching which is not penalised in surfactant type systems: The chain stretching required in polymer systems to fill network nodes with more than 3 connectors becomes prohibitive for the formation of those phases unless alleviated by the addition of shorter homopolymers chains or some kind of nanoparticle which can reside in the nodal centers as space fillers [13, 14].

However, as illustrated above with the AB_2 miktoarm stars a change in molecular architecture can induce increased interfacial curvature and stabilise new phases. In Fig. 10.5 a simulated phase diagram is shown of $A(BC)_2$ miktoarm star melts. A reference structure where each chain is roughly the same length assembles to a perforated lamellae structure (verified experimentally in [15]) and as each arm length is varied relative to that a number of new structures appear on the periphery of the perforated lamellae region. First, as the A arm is shortened, a single gyroid phase emerges (GL_{AB}) - note that this is a chiral structure - while for longer A arms a double diamond phase is stabilised. Increasing the middle B-block leads to a hybrid structure with the red A component forming a spherical packing while the green C species forms a 3-connected gyroid-like network. Note that because of the multicomponent nature of the molecules, the middle B blocks in these phases form topologically very complex continuous morphologies with channels and cavities.

As mentioned above, a unifying feature between the structures formed in the linear AB and ABC systems shown in Fig. 10.1 is that they are all characterised by the interfaces of each pair of polymer species. Although the $A(BC)_2$ miktoarm stars allow the formation of a range of topologically complex phases, they can still effectively be though of as a linear ABC molecule only with added splay due to the two diblock chains. This is because the topology of the star branch point only involves two of the chain species and so effectively acts in the same way as the connection of a linear molecule. However, another option when adding a third component is to make a star-like topology where all species meet at the branch point. Such molecules are called ABC miktoarm star terpolymers (Fig. 10.1). The self-assembly behaviour of ABC stars have been investigated experimentally [17] and theoretically [18, 21–23]. The generic theoretical phase diagram as described by these sources is shown in Fig. 10.6 under the compositional constraint of two components occupying equal volume fractions and of symmetric interaction parameters between the different polymer species. Compared with the self-assembly of linear block copolymers a fundamental result appears despite these severe constraints: dictated by the molecular star topology ABC lines are formed where the three different interfaces between AB, AC and BC meet [18–21]. As a consequence, a sequence of columnar structures with cross-sections following various polygonal tiling patterns appears. This sequence of

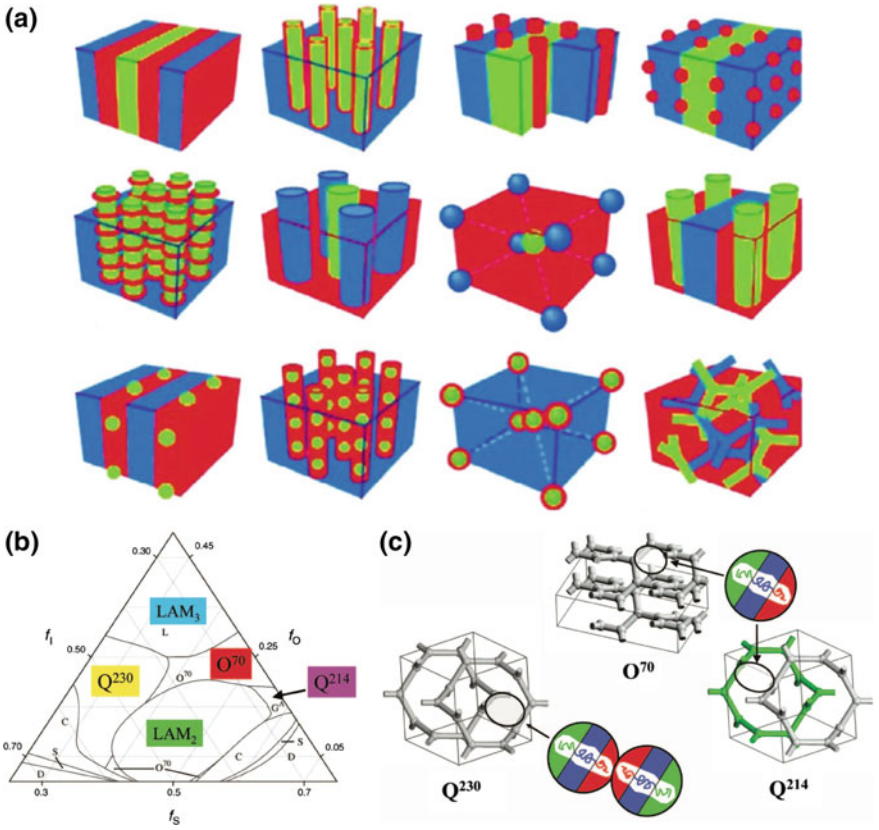

Fig. 10.4 Linear ABC triblock copolymer phases. **a** A selection of structures formed in linear ABC systems. Figure from [11]. **b** Theoretical ternary phase diagram showing the appearance of three different 3-connected network phases [12], the orthorhombic O^{70} phase and the two cubic double gyroid phases Q^{230} and Q^{214}. **c** Network representations and local molecular configurations of the networks from **b**. Figures (b, c) from [12]

tilings has been predicted from all the earlier mentioned theoretical studies and has been found in a number of experimental ABC 3-miktoarm star terpolymer systems [17].

Again, one can influence the interfacial curvature by altering the molecular architecture. In Fig. 10.7 the composition of ABC stars is altered by adding chains of equal length instead of increasing the length of one chain. Direct comparison with the ABC star phase diagram in Fig. 10.6 shows that the tiling patterns at $x = 2$ and $x = 3$ are now replaced with new decorations of the bicontinuous motifs of the diamond and gyroid network patterns. In these new structures one of the two nets are now built from alternating globular domains of the minority components. The striped double diamond has been found experimentally in a blend system as described below [24].

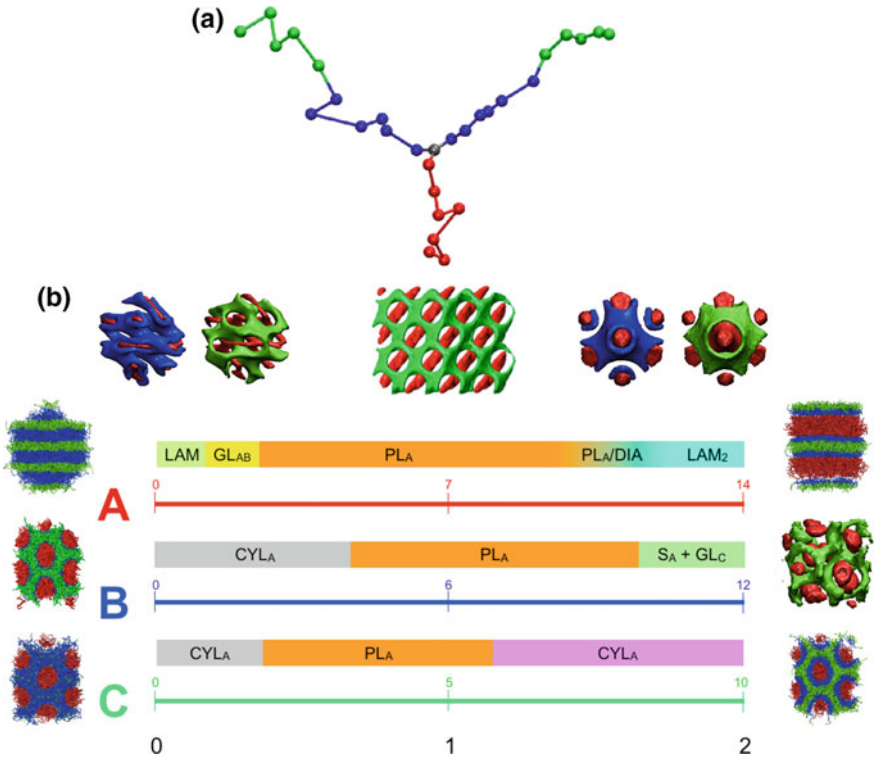

Fig. 10.5 **a** $A(BC)_2$ miktoarm star. **b** Simulated phase diagram of $A(BC)_2$ miktoarm stars from [16]

As mentioned above, the connectivity of ABC stars sets a topological constraint on the possible self-assembly morphologies but also leads to new possibilities. One very exciting option set forth by Hyde and co-workers is the formation of new tri- and polycontinuous patterns [20, 25]. They showed that such patterns were topologically consistent with the star molecular architecture and hypothesised their formation in star systems. A number of candidate structures were suggested (see Fig. 10.8) and evaluated in terms of energetics but any of them remains to be found experimentally in an ABC star system.[2] However, by suitably adjusting the molecular architecture and chemistry of ABC stars it turns out one can favour a thermodynamically stable tricontinuous structure based on three intertwined so-called ths-nets as was demonstrated using self-consistent field theory in [28] (see Fig. 10.9). This is a spectacular network structure effectively carving up space into three separated congruent labyrinths, each

[2]One of the predicted tricontinuous patterns have in fact been identified in both a hard and a soft matter context. In [26] such a pattern was found in a mesoporous silica and the same structure was later identified in a lyotropic liquid crystalline surfactant system [27]. However, in those cases the channels all contain the same material unlike the structures described here which have a different chemical species inside each channel.

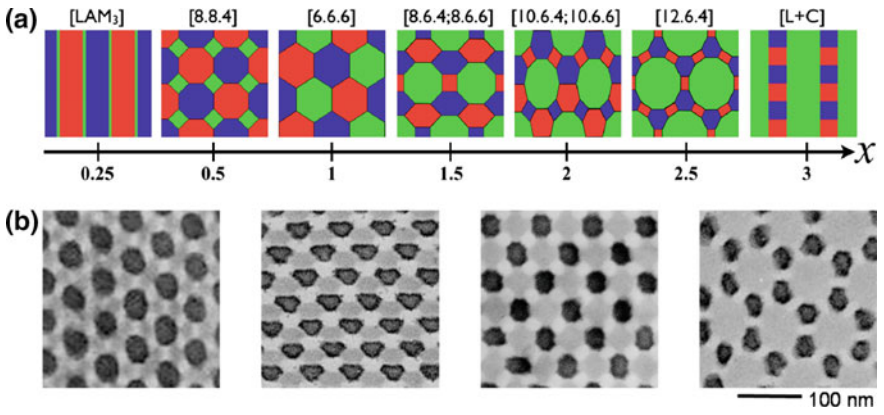

Fig. 10.6 **a** Generic phase diagram for ABC 3-miktoarm star terpolymers. The A and B components are constrained to occupy equal volume fractions and interactions between all unlike components are symmetric [18, 21–23]. The different phases are placed at their approximate compositional positions quantified by the parameter x, the volume ratio of the C and A (= B) components. The tilings are denoted by their Schläfli symbol [18, 21], a set of numbers $[k_1.k_2.\ldots.k_l]$ indicating that a vertex is surrounded by a k_1-gon, a k_2-gon,…in cyclic order. Tilings with more than one topologically distinct vertex are named as $[k_1.k_2.k_3; k_4.k_5.k_6]$. Color code: A: red, B: blue, C: green. **b** Examples of tiling patterns from poly(isoprene-b-styrene-b-2-vinylpyridine) miktoarm star terpolymers visualized by transmission electron microscopy. Images from [17]

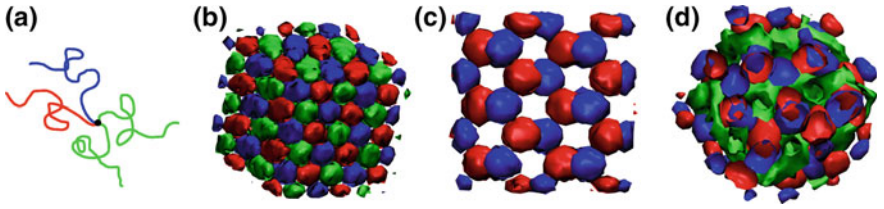

Fig. 10.7 Varying the composition by adding chains of equal length instead of increasing the length of one chain results in completely new structures [23]. **a** An ABC_2 star ($x = 2$). **b** For $x = 1$ the result is still the [6.6.6] tiling. **c** For $x = 2$ a double diamond network structure is found with one net built from alternating A and B domains. **d** For $x = 3$ the system also forms a striped network structure but now with the topology of the double gyroid structure with one net built from alternating red and blue domains. Figures from [23]

with a separate chemistry and thus properties. The key to stabilising this structure stems from the introduction of an extended core which effectively alters the balance between entropic and enthalpic free energy contributions, ultimately allowing this new pattern to outfavour the prismatic hexagonal honeycomb.

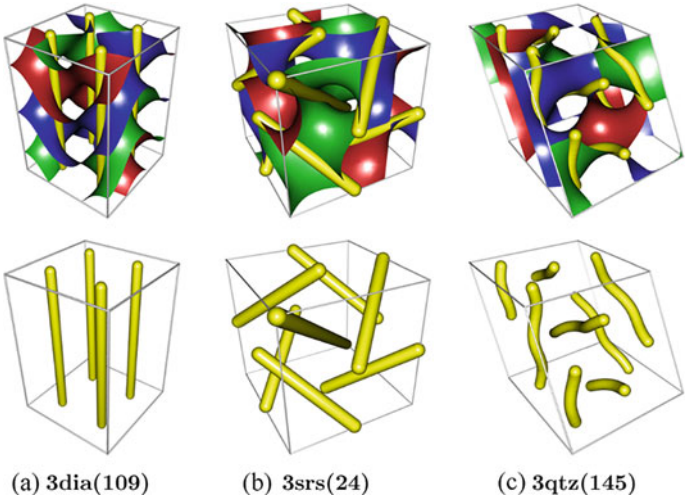

Fig. 10.8 Examples of tricontinuous candidate patterns topologically consistent with the star molecular architecture [20]. Yellow lines indicate the triple lines along which the star molecular cores pack. **a** 3 intertwined diamond nets. **b** 3 intertwined gyroidal srs-nets (all of same handedness, so a chiral structure). **c** 3 intertwined quartz qtz-nets (also chiral). Figure from [28]

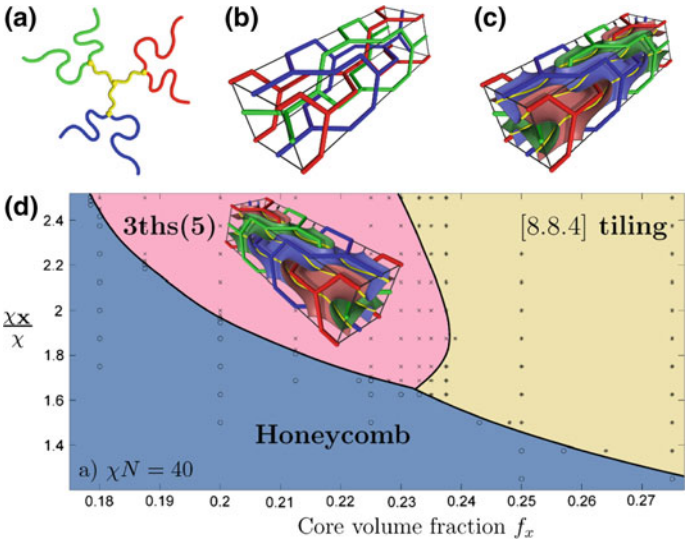

Fig. 10.9 **a** A dual chain core ABC star triblock copolymer. **b** Triply intergrown *ths*-nets. **c** As in **b** but showing the interfaces also. **d** Phase diagram from [28]: As a function of the core volume fraction and the interaction strength three structures dominate the phase diagram, one of which is a spectacular tricontinous network structure

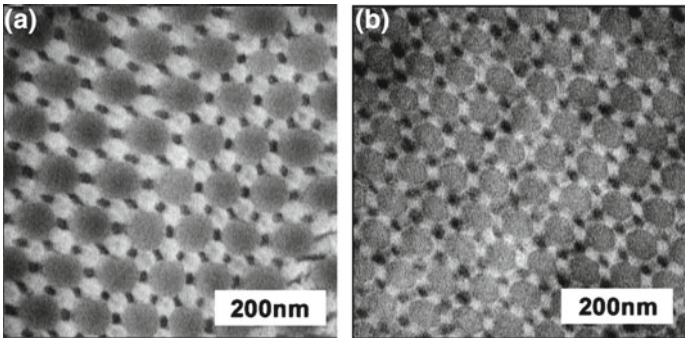

Fig. 10.10 Blending block copolymers. **a** An asymmetric polystyrene-b-polybutadiene-b-poly(2-vinylpyridine) ($S_{34}B_{11}V_{55}$) miktoarm star terpolymer forms a [12.6.4] tiling on its own (subscripts indicate molecular weight). The minority B component forms the dark 4-sided domains while the S component forms the white hexagonal domains in the tiling. **b** When blended with a $S_{45}V_{55}$ diblock copolymer the tiling pattern remains [12.6.4] but the chemical nature of the hexagons and squares swap so that B now forms hexagons and S forms squares. Figures from [29]

10.4 Blending Molecular Architectures

Blending polymers has been a heavily used strategy for many years to obtain a material with new properties akin to alloys in metallurgy. This also applies to block copolymers where one approach is to swell a particular domain with shorter homopolymer chains of the same species - in analogy to swelling in lyotropic liquid crystalline systems. For example, blending an ABC star which alone forms the [6.6.6] tiling pattern with C homopolymer chains can lead to a zinc-blende structure with alternating AB domains building up a diamond network [24] as the one illustrated in Fig. 10.7c above. If the swelling agent is not a homopolymer chain but another block copolymer, compatibility between pairs of blocks of both molecules becomes another control parameter for structure formation. An example is shown in Fig. 10.10 where blending an ABC star which forms the [12.6.4] tiling alone with AB diblock copolymers causes the A and B components to swap polygonal symmetry positions in the tiling pattern [29]. Thus, blending opens up the possibility of fine-tuning the structures found in the pure systems or allowing completely new patterns to appear. However, the possible phase space of a blend of different block copolymers stars is enormous. The main variables in play are (i) the molecular topology, i.e. the connectivity of the chains, (ii) the composition, i.e. the volume fractions of the different chains including the blend ratio, (iii) the chemical nature of the different polymer species, i.e. their mutual interaction parameters. Secondary variables can be polydispersity of the chains and chain flexibility for example [1].

In Fig. 10.11 an example is shown where a series of spectacular structures are predicted to form in blends of two different miktoarm stars [30]. Blending ABC and ABD star triblocks in a 50/50 ratio and with the majority domains (green C + yellow D) 2–7 times longer than the minority components (red A + blue B) a series

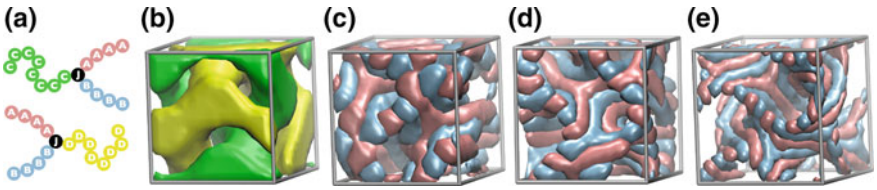

Fig. 10.11 **a** Blending ABC and ABD 3-miktoarm star terpolymers. All molecules contain equal sized A (red) and B (blue) arms, and longer C (green) and D (yellow) arms, but also of equal size. The parameter x (equal to $8/4 = 2$ in this image), corresponds to the number ratio of C to A beads. **b** C and D domain geometry, a pair of intertwined gyroid nets. **c–g** Single unit cell snapshots illustrating the curved striped pattern formed by the minority components A and B for varying x. **c** $x = 2$, **d** $x = 3.67$, **e** $x = 6$. Note the 3-fold branching for all values of x. Figures from [30]

of complex chiral network structures are predicted to form. The C and D species form two chiral enantiomeric nets separated by a membrane following the gyroid surface. As the C and D chains grow, the overall structure remains a chiral gyroid, but unlike all hitherto found gyroid(-like) structures, the channels in these new structures constitute majority domains resulting in the formation of a thin hyperbolic film.

Depending on the composition, interactions and molecular architectures in play, the minority components form remarkable structures on this hyperbolic curved film, in particular ordered branched structures which can be thought of as 'hyperbolic lamellae'. It is important to realise that if the film was flat, regular lamellae would form, but because of the curvature of the film branching has to occur. Remarkably, it turns out that these branched patterns are theoretically related to a family of tilings in the hyperbolic plane which when embedded on the gyroid surface yields distinct interwoven chiral nets, always of the same handedness and which changes topology systematically as a function of composition. The non-chiral nature of the block copolymer preclude a preferred handedness, which in the numerical simulations results in domains of opposite chirality forming, ultimately giving rise to defects, see Fig. 10.12. Nevertheless, the ideal mesostructures of these patterns in three-dimensional space are spectacular and extraordinarily complex. The minority components form multiple threaded chiral nets (all of equal handedness) whose topologies are that of the gyroid net. The number of disjoint nets making up the hyperbolic film can be up to 54 [30]. These intricate self-assemblies of liquid-like domains thus rival the complex interwoven networks found in synthetic metal-organic frameworks [31].

10.5 Concluding Remarks

The role of molecular architecture (chain topology) has been shown to be a defining variable influencing the resulting self-assembly morphologies in block copolymer melts and a number of patterns with complex topology has been presented from

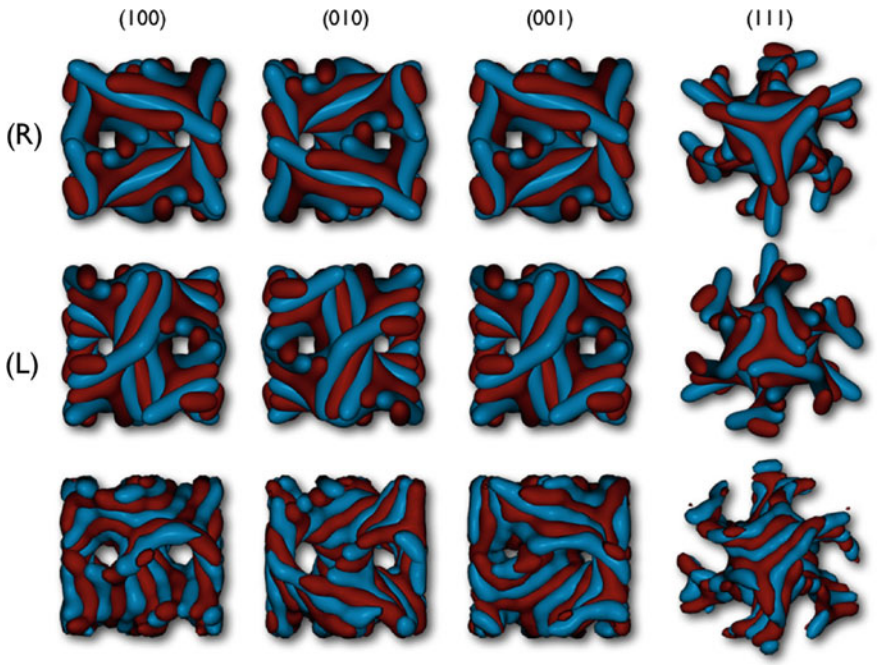

Fig. 10.12 Comparison of ideal left- (L) and right-handed (R) patterns (top and middle rows) viewed from various directions with a self-assembled morphology formed in a simulated mixture of terpolymers with $x = 4$ (bottom row). The simulated morphologies can be seen to match both of the ideal left- and right-handed patterns in distinct patches of the unit cell and are therefore of mixed chirality

experiments and simulations. From a topological perspective perhaps the simplest way to condense the message presented here is shown in Fig. 10.13. Here symmetric AB diblocks are compared as a 2-star with an ABC 3-star and a ABCD 4-star and it is clear that the interfacial dimensionality changes as the molecular topology is altered. Each pair of species defines a surface and as the surfaces have to meet in space we go from 2D interfaces to 1D line interfaces and finally to 0D point interfaces in a cellular packing. In the latter case, Monte Carlo simulations of symmetric ABCD 4-miktoarm stars by Dotera [32] showed that a 4-colored Kelvin foam was the optimal packing, and not for example a square 4-colored tiling pattern.

As the molecular composition is altered away from the symmetric case, the resulting structural response becomes a combination of these motifs as illustrated in Fig. 10.14. Here an asymmetric ABCD star is shown to form a hexagonal columnar structure with elements of a [12.6.4] tiling along the cylinder axis, but apart from the cylinders themselves remains a cellular structure. Many more structures are expected to be found in these and higher order block copolymer molecules as combinations of the topologies displayed here. From a theoretical perspective we can continue to add chains but the synthetic community is in some sense way ahead of theory:

In Fig. 10.15 a range of examples are shown of incredible molecular architectures synthesised in the group of A. Hirao. The potential morphologies and topologies to be found in these systems is unknown as these molecules are still largely unexplored structurally both theoretically and experimentally.

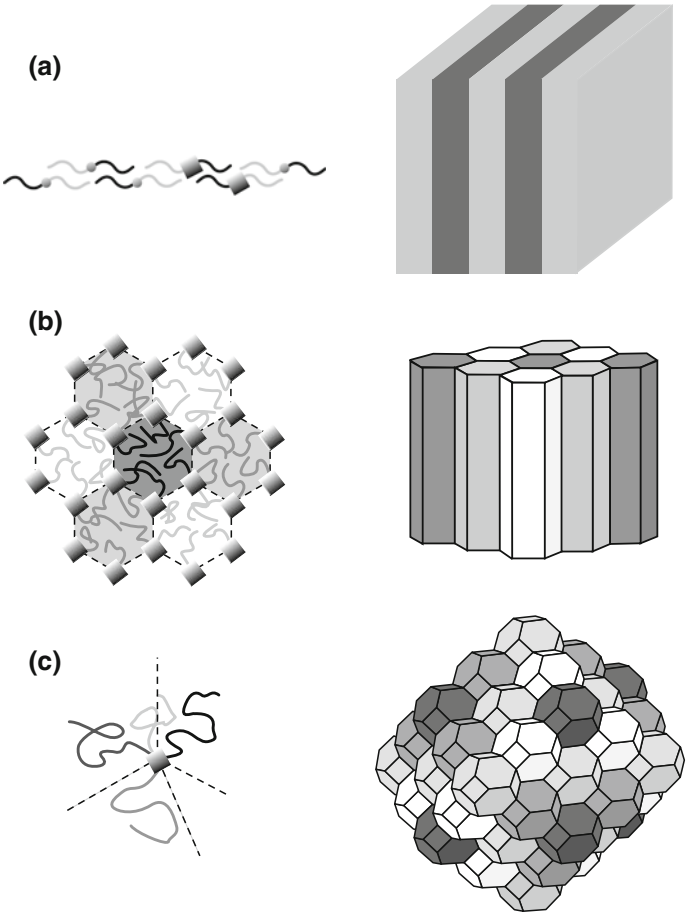

Fig. 10.13 The mutual interfacial dimensionality changes with the molecular architecture for symmetric block copolymers. **a** Diblocks form lamellae with 2D (surface) interfaces. **b** ABC star triblocks form tiling patterns with 2D and 1D (line) interfaces. **c** ABCD star tetrablocks form cellular packings with 2D, 1D and 0D (point) interfaces. This particular cellular packing is a 4-colored Kelvin foam, i.e. each component forms a closed cell in the shape of a truncated octahedron surrounded by 14 neighbors. This structure has been predicted to form in symmetric ABCD stars [32]. Figure from [32]

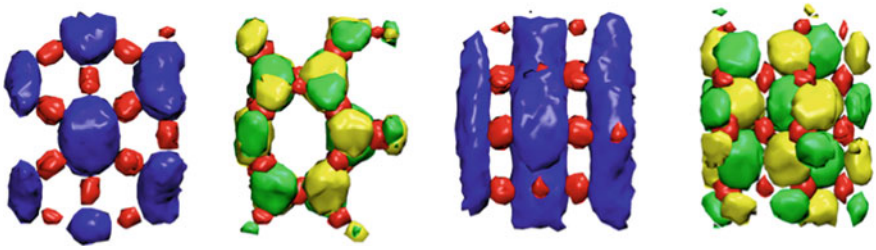

Fig. 10.14 Edge-on (left) and top-down (right) split views of morphology formed in an asymmetric four-armed ABCD miktoarm star with arm length ratios of 1:4:2:2. Color code: A (red), B (blue), C (green), D: (yellow)

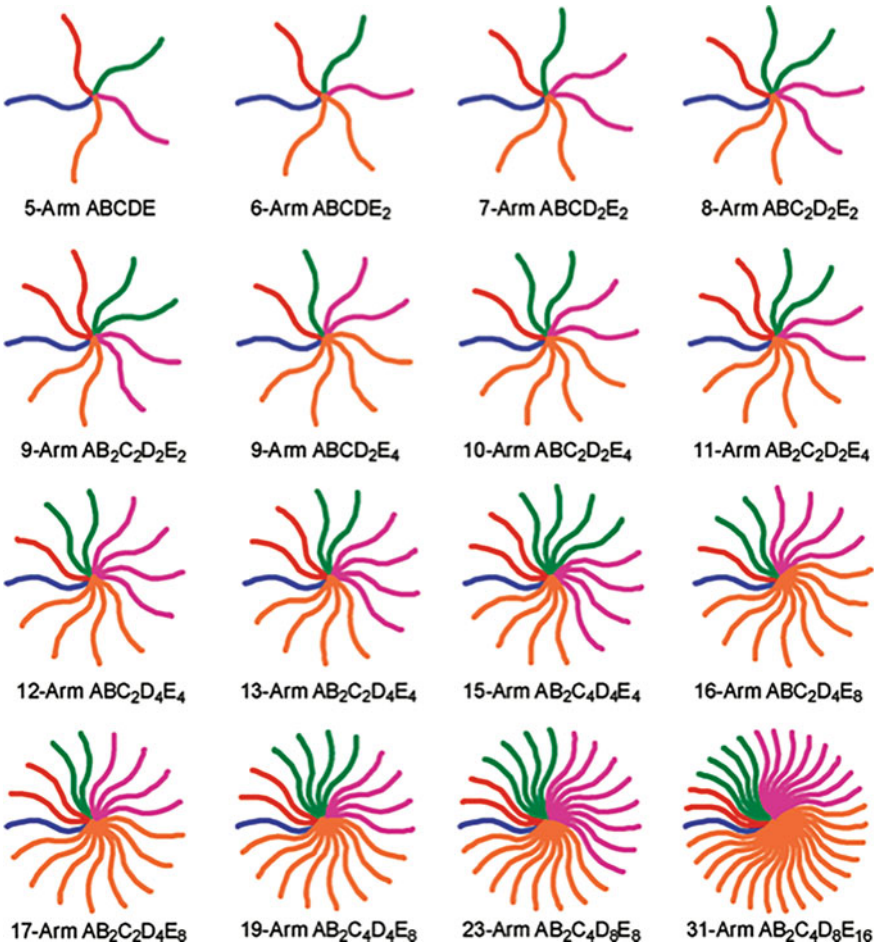

Fig. 10.15 A selection of possible structures of asymmetric star polymers obtained by Hirao and co-workers using advanced iterative synthetic techniques. Figure from [33]

Acknowledgements The author wishes to gratefully acknowledge colleagues and mutual co-authors of the authors own research presented in this chapter, in particular Stephen T. Hyde, Liliana de Campo, Myfanwy Evans, Martin C. Pedersen, Gerd E. Schröder-Turk, Michael G. Fischer, Panagiota Fragouli, Nikos Hadjichristidis and Kell Mortensen.

References

1. F. Bates, M. Hillmyer, T. Lodge, C. Bates, K. Delaney, G. Fredrickson, Science **336**, 434–440 (2012)
2. N.A. Lynd, A.J. Meuler, M.A. Hillmyer, Prog. Polym. Sci. **33**, 875–893 (2008)
3. M. Matsen, Macromolecules **45**, 2161–2165 (2012)
4. M. Huggins, J. Chem. Phys. **9**(5), 440 (1941)
5. P. Flory, J. Chem. Phys. **10**, 51 (1942)
6. S.T. Hyde, in *Handbook of Applied Surface and Colloid Chemistry*, ed. by K. Holmberg (Wiley, 2001); chapter 16
7. C. Huang, H. Yu, Polymer **48**, 4537–4546 (2007)
8. S. Lee, M. Bluemle, F. Bates, Science **330**, 349–353 (2010)
9. S. Kim, K. Jeong, A. Yethiraj, M. Mahanthappa, Proc. Natl. Acad. Sci. USA **114**(16), 4072–4077 (2017). https://doi.org/10.1073/pnas.1701608114
10. T. Gillard, S. Lee, F. Bates, Proc. Natl. Acad. Sci. USA **113**(19), 167–5172 (2016)
11. N. Hadjichristidis, H. Iatrou, M. Pitsikalis, S. Pispas, A. Avgeropoulos, Prog. Polym. Sci. **30**, 725–782 (2005)
12. F. Bates, MRS Bull. **30**, 525–532 (2005)
13. F. Martinez-Veracoechea, F. Escobedo, Macromolecules **40**, 7354–7365 (2007)
14. P. Padmanabhan, E. Martinez-Veracoechea, F. Escobedo, Macromolecules **49**, 5232–5243 (2016)
15. J.J.K. Kirkensgaard, P. Fragouli, N. Hadjichristidis, K. Mortensen, Macromolecules **44**(3), 575–582 (2011)
16. J.J.K. Kirkensgaard, Soft Matter **6**, 6102–6108 (2010)
17. Y. Matsushita, K. Hayashida, T. Dotera, A. Takano, J. Phys. Condens. Matter **23**, 284111 (2011)
18. T. Gemma, A. Hatano, T. Dotera, Macromolecules **35**, 3225–3227 (2002)
19. J.J.K. Kirkensgaard, S. Hyde, Phys. Chem. Chem. Phys. **11**, 2016–2022 (2009)
20. S.T. Hyde, L. de Campo, C. Oguey, Soft Matter **5**, 2782–2794 (2009)
21. J.J.K. Kirkensgaard, M.C. Pedersen, S.T. Hyde, Soft Matter **10**, 7182–7194 (2014)
22. C.-I. Huang, H.-K. Fang, C.-H. Lin, Phys. Rev. E **77**, 031804 (2008)
23. J.J.K. Kirkensgaard, Phys. Rev. E **85**, 031802 (2012)
24. K. Hayashida, A. Takano, T. Dotera, Y. Matsushita, Macromolecules **41**, 6269–6271 (2008)
25. S. Hyde, G. Schröder, Curr. Opin. Colloid Interface Sci. **8** (2003),
26. Y. Han, D. Zhang, L. Chng, J. Sun, L. Zhao, X. Zou, J. Ying, Nat. Chem. **1**, 123–127 (2009)
27. G. Sorenson, A. Schmitt, M. Mahanthappa, Soft Matter **10**, 8229–8235 (2014)
28. M. Fischer, L. de Campo, J. Kirkensgaard, S. Hyde, G. Schröder-Turk, Macromolecules **47**, 7424–7430 (2014)
29. V. Abetz, S. Jiang, e-Polymers **054**, 1–9 (2004)
30. J. Kirkensgaard, M. Evans, L. de Campo, S. Hyde, Proc. Natl. Acad. Sci. USA **111**(4), 1271–1276 (2014)
31. L. Carlucci, G. Ciani, D. Proserpio, Coord. Chem. Rev. 247–289 (2003)
32. T. Dotera, Phys. Rev. Lett. **82**(1), 105 (1999)
33. T. Higashihara, T. Sakurai, A. Hirao, Macromolecules **42**, 6006–6014 (2009)